ARTICLE

# Room Temperature Magnetic Behavior of Sol-Gel Synthesized Mn Doped ZnO

Murtaza Saleem[a], Saadat A. Siddiqi[a*], Shahid Atiq[b], M. Sabieh Anwar[b], Saira Riaz[a]

*a. Centre for Solid State Physics, University of the Punjab, Quaid-e-Azam Campus, Lahore-54590, Pakistan*

*b. School of Science and Engineering, Lahore University of Management Sciences, Opposite Sector U, D.H.A. Lahore-54792, Pakistan*

(Dated: Received on April 11, 2010; Accepted on June 3, 2010)

Mn doped ZnO nano-crystallites were synthesized by state of the art sol-gel derived auto-combustion technique. As-burnt powder was investigated with different characterization techniques to explore the properties of Mn doped ZnO dilute magnetic semiconductor. X-ray diffraction measurements indicate that Mn doped ZnO retain wurtzite type hexagonal crystal structure like ZnO. Compositional and morphological studies were carried out by energy dispersive X-ray analysis and scanning electron microscopy, respectively. Temperature dependent resistivity of the sample exhibited the semiconducting behavior of the DMS material. Room temperature magnetic properties determined by vibrating sample magnetometer, revealed the presence of ferromagnetic and diamagnetic contributions in Mn doped ZnO.

**Key words:** Nanocrystal, Diluted magnetic semiconductor, Auto-combustion, Room temperature ferromagnetism

## I. INTRODUCTION

Partial substitution of magnetic ions in non magnetic semiconductors produce diluted magnetic semiconductors (DMSs) [1, 2]. ZnO is a direct band-gap ($E_g$=3.37 eV) semiconductor with a wurtzite type hexagonal crystal structure. ZnO-based transition metals doped DMS materials have successfully been synthesized by some research groups [3, 4]. Ferromagnetic properties of Mn doped ZnO in bulk and thin film forms have recently been investigated [5, 6]. $Zn_{1-x}Mn_xO$ ($x$=0.1 and 0.3) thin films grown on $Al_2O_3$ substrates by laser molecular beam epitaxy (MBE) have been reported to show a $T_c$ value in the 30–40 K range [7], whereas films of similar compositions have also been reported to exhibit spin-glass behavior with a strong antiferromagnetic exchange coupling by Fukumura *et al.* [8]. Kim *et al.* observed Curie temperature $T_C \approx 39$ K in $Zn_{0.8}Mn_{0.2}O$ films synthesized by sol gel method [9]. Similarly, interesting results have also been reported on bulk samples. For example, Han *et al.* reported a ferrimagnetic phase transition in the case of $Zn_{0.95}Mn_{0.05}O$ sample processed at 1170 K attributed to the presence of the impurity spinel phase (Mn, Zn) $Mn_2O_4$ in the system [10]. Similar results were obtained by Li *et al.* in sol-gel derived $Zn_{1-x}Mn_xO$ samples sintered in nitrogen atmosphere at 900 °C [11]. Sharma *et al.* investigated room temperature ferromagnetism in low temperature processed bulk and thin films of Mn-doped ZnO [12]. Recently, Chen *et al.* have studied the effect of sintering temperature on the magnetic properties of Mn-doped ZnO [13]. Sharma *et al.* observed ferromagnetic interaction in the samples sintered below 700 °C in Ar atmosphere and found that ferromagnetic behavior disappeared when samples were sintered in air [14].

Room temperature ferromagnetism in DMS materials has immense significance from the application point of view. It is observed that magnetic behavior in Mn doped ZnO is strongly dependent on the modes of preparation conditions. The sol-gel derived auto-combustion technique is a simple, fast, and reliable method with many other unique synthesis advantages. During the reaction, gel is prepared and subsequently, an auto-combustive self-propagation reaction ensures crystallization and oxide formation, producing the required phases in a short period of time [3, 15].

In this work, nanocrystallites of Mn doped ZnO have been synthesized using sol-gel derived auto combustion technique. This method is believed to be fruitfully flexible in achieving a homogeneous single-phase material. Structural, morphological, electrical, and magnetic properties of the sol-gel synthesized DMS material have been explored.

*Author to whom correspondence should be addressed. E-mail: murtaza092@yahoo.com, Tel.: +92-300-8794801, FAX: +92-42-9231139

 

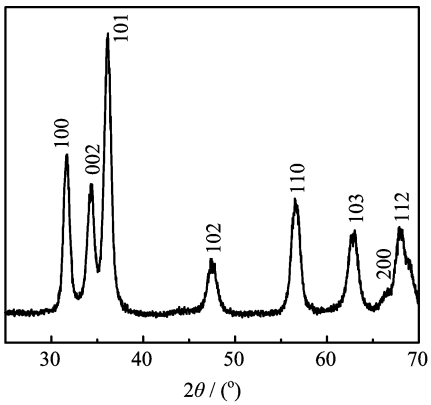


FIG. 1 XRD spectrum of $Zn_{0.95}Mn_{0.05}O$.

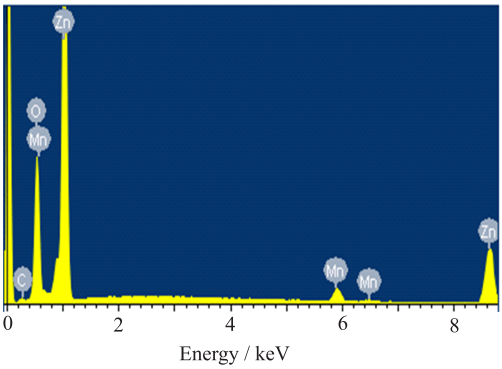


FIG. 2 EDX spectrum of $Zn_{0.95}Mn_{0.05}O$.

## II. EXPERIMENTS

For the preparation of $Zn_{0.95}Mn_{0.05}O$, appropriate molar ratios of Zn nitrate ($Zn(NO_3)_2{\cdot}6H_2O$), Mn nitrate ($Mn(NO_3)_2{\cdot}6H_2O$), and citric acid ($C_6H_8O_7$) were dissolved in 100 mL distilled water. All the chemicals had contents of analytical grade purity. Metal nitrates (MN) to citric acid (CA), with a molar ratio of 1:1, were taken. Initial pH of the solution was observed between 2.5 and 3.5, which was kept at 7 by adding proper amount of liquid ammonia $NH_3$. The solution was dried at 150 °C under constant stirring to obtain xerogel. The temperature was increased to 250 °C after attaining the xerogel and this gel was converted into powder by a self combustive exothermic reaction.

The resulting as-synthesized powder was characterized by X-ray diffraction (XRD) using a Panalytical X'Pert Pro multipurpose diffractometer (MPD) for the crystallographic measurements. The X-ray diffractometer was operated at 40 kV and 40 mA with Cu K$\alpha$ radiation ($\lambda$=1.540598 Å). Energy dispersive X-ray (EDX) analysis has been carried out by an S-3700N (Hitachi, Japan) and scanning electron microscopy (SEM) for compositional and micro-structural studies, respectively. JEOL SEM has been used in its secondary electron image (SEI) mode operated at 5 kV to avoid any charging effect on the surface. Some amount of the powder was pelletized to measure the temperature dependent resistivity measurements for electrical properties. The magnetic properties of the powder sample were performed by vibrating sample magnetometry (VSM) by Lakeshore-7404.

## III. RESULTS AND DISCUSSION

There is usually no disturbance in the wurtzite type hexagonal structure of ZnO, when it is doped with small amounts of impurity elements [16]. The XRD pattern (Fig.1) also shows that Mn substitution does not disturb the hexagonal wurtzite type crystal structure of the host ZnO. Mn doping into ZnO matrix is evident from the peak broadening to a considerable extent. In general, the sample was observed to have a pure single phase characteristic wurtzite type hexagonal structure of the ZnO based diluted magnetic semiconductor. The lattice parameters $a$ and $c$ of the rather complex wurtzite structure were determined using "CELL". The calculated values of $a$ and $c$ were 3.2471 and 5.2011 Å, respectively. The estimated crystallite size was calculated by considering the most intense diffraction peak (101) in the pattern using well known Scherrer formula [3],

$$D_{hkl} = \frac{k\lambda}{\Delta\theta\cos\theta} \tag{1}$$

where $\theta$ is Bragg's angle in degree, $D_{hkl}$ denotes the average crystallite diameter, $k$ is a constant ($k$=0.94), $\lambda$ depicts the wavelength of 0.154 nm of the Cu K$\alpha$ radiation and $\Delta\theta$ the half maximum line width in radians. The crystallite size of the sample was evaluated approximately as 37 nm.

EDX analysis performed for the composition confirmation showed that the stoichiometric amounts of Zn, Mn, and O elements were present in the as-synthesized $Zn_{0.95}Mn_{0.05}O$ sample, as shown in Fig.2. The EDX pattern confirmed the incorporation of Mn in the ZnO structure and the percentage was very nearly equal to the nominal value of Mn in ZnO. This revealed the phase purity of the sample, however, traces of small percentage of carbon were also observed and can be attributed to the sample stub.

JEOL SEM was used to study the morphology of the powder sample. Figure 3 shows the SEM micrograph of the ZnMnO sample. One can see a good proportion of the grains having small grain size. Whereas, very large agglomerates are also present that can be collimated up to a lesser extent. The grains have well-defined shapes and edges. The SEM image usually gives the grain size while the XRD measurements provide an estimate of the size of crystallites. It is very difficult to correlate both the results exactly because the crystallite size is hard to deduce from the SEM image. High quality crystallinity

DOI:10.1088/1674-0068/23/04/469-472 

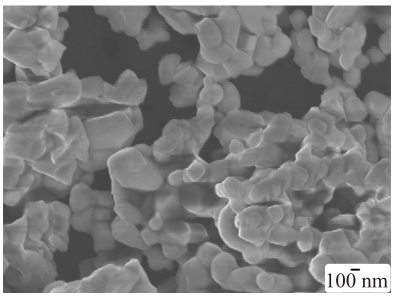


FIG. 3 SEM micrograph of $Zn_{0.95}Mn_{0.05}O$.

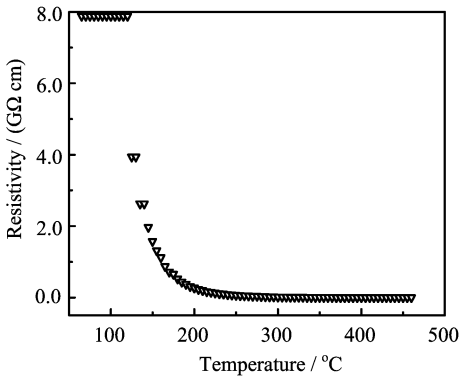


FIG. 4 Temperature-dependent DC electrical resistivity of $Zn_{0.95}Mn_{0.05}O$.

and uniformity may not be seen from the SEM image, however phase purity of the sample can be deduced from the compositional analysis carried out by EDX analysis. The temperature-dependent DC electrical resistivity of the $Zn_{0.95}Mn_{0.05}O$ sample was evaluated by using a two point probe set up. Temperature-dependent volume resistance $R_v$ of the sample was measured and the corresponding values of resistivity were calculated using the relation [17],

$$\rho_v = \frac{R_v A}{L} \tag{2}$$

where, $\rho_v$ is volume resistivity, $R_v$ is the measured volume resistance, $A$ is the total area of the sample and $L$ is the thickness of the pellet. The values of temperature-dependent DC electrical resistivity evaluated for the sample is shown in Fig.4. The overall trend observed in the sample was that the value of DC electrical resistivity decreased with the increase of temperature, confirming the semiconductor behavior of the prepared diluted magnetic semiconductor.

Magnetic hysteresis (M-H) loop of the sample was obtained up to magnetic field range ±15 kOe at room temperature as the result is depicted in Fig.5, indicating ferromagnetic behavior. Origin of magnetism in DMS materials has remained in controversy since long. According to RKKY theory, the ferromagnetic behavior in DMS material arises as a result of the exchange interaction between local spin-polarized electrons (such

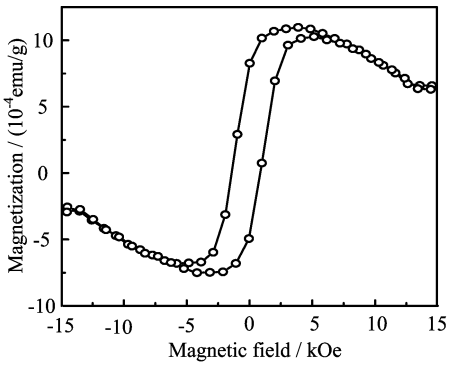


FIG. 5 Field dependent magnetization of $Zn_{0.95}Mn_{0.05}O$.

as the electrons of $Mn^{2+}$) and conductive electrons [14, 18]. The saturation magnetization obtained from M-H curve was observed as $11\times10^{-4}$ emu/g. Sharma *et al.* reported that the lower values of saturation magnetization might be due to the smaller sizes of crystallites in the samples [14]. Kim *et. al.* reported very high coercivity values of ZnMnO [9]. Similar behavior can be seen in our results. Magnetic behavior of the same material might be rather different when it was investigated in powder, bulk or thin film forms. This effect arises due to the dependence of magnetic behavior on the structural arrangement. When the material is investigated in powder form, the surface of every particle behaves independently and is influenced strongly by the other neighboring particles. Consequently, the disturbance in magnetic interactions can be observed due to this surface and inter-particle boundary connections. The parent ZnO material contains diamagnetic behavior and Mn only partially substitutes the ZnO sites in case of DMS materials, therefore, Mn doped ZnO indicates magnetic behavior with ferromagnetic and diamagnetic contributions at room temperature. The diamagnetic contributions were observed in the sample, especially at higher applied fields, and also be attributed by the sample holder [19] and parent ZnO material. These diamagnetic contributions cause the decrease in magnetization in our sample in the field range of 5–15 kOe, revealing the field opposing behavior.

## IV. CONCLUSION

Sol-gel synthesized $Zn_{0.95}Mn_{0.05}O$ sample was characterized by XRD, EDX, SEM, temperature dependent resistivity, and VSM for the study of structural, compositional, morphological, electrical and magnetic properties, respectively. XRD pattern of $Zn_{0.95}Mn_{0.05}O$ with broadened peaks due to Mn substitution indicates the wurtzite type hexagonal structure like ZnO. No second or impurity phase was detected. EDX analysis confirmed the compositional purity of the elements contained in the sample. Phase pure morphology of the

DOI:10.1088/1674-0068/23/04/469-472 

sample was demonstrated by the SEM micrographs. Characteristic semiconducting behavior of the sample was revealed by the temperature dependent resistivity measurements. Net influx of diamagnetic and ferromagnetic contributions was observed. In general, room temperature ferromagnetic behavior was successfully achieved in sol-gel synthesized Mn doped ZnO material.

## V. ACKNOWLEDGMENTS

This work was supported by the Higher Education Commission (HEC), Pakistan to indigenous Ph. D. students. We are grateful to Dr. Riaz Ahmad, Department of Physics, GC University, Lahore, Pakistan for providing XRD facility.

[1] X. C. Liu, E. W. Shi, Z. Z. Chen, T. Zhang, Y. Zhang, B. Y. Chen, W. Huang, X. Liu, L. X. Song, K. J. Zhou, and M. Q. Cui, Appl. Phys. Lett. **92**, 042502 (2008).
[2] Y. J. Lin, C. L. Tsai, W. C. Chen, C. J. Liu , L. Horng, Y. T. Shih, Z. R. Lin, and J. F. Wang, J. Cryst. Growth **310**, 3763 (2008).
[3] G. Pei, F. Wu, C. Xia, J. Zhang, X. Li, and J. Xu, Curr. Appl. Phys. **8**, 18 (2008).
[4] C. Cheng, G. Xu, H. Zhang, Y. Luo, and Y. Li, Mater. Lett. **62**, 3733 (2008).
[5] D. C. Kundaliya, S. B. Ogale, S. E. Lofland, S. Dhar, C. J. Metting, S. R. Shinde, Z. Ma, B. Varughese, K. V. Ramanujachary, L. Salamanca-Riba, and T. Venkatesan, Nature Mater. **3**, 673 (2004).
[6] S. W. Lim, M. C. Jeong, M. H. Ham, and J. M. Myoung, Jpn. J. Appl. Phys. **43**, L280 (2004).
[7] S. W. Jung, S. J. An, G. C. Yi, C. U. Jung, S. Lee, and S. Cho, Appl. Phys. Lett. **80**, 4561 (2002).
[8] T. Fukumura, Z. Jin, M. Kawasaki, T. Shono, T. Hasegawa, S. Koshihara, and H. Koinuma, Appl. Phys. Lett. **78**, 958 (2001).
[9] Y. M. Kim, M. Yoon, I. W. Park, Y. J. Park, and J. H. Lyou, Solid State Commun. **129**, 175 (2004).
[10] S. J. Han, T. H. Jang, Y. B. Kim, B. G. Park, J. H. Park, and Y. H. Jeong, Appl. Phys. Lett. **83**, 920 (2003).
[11] J. H. Li, D. Z. Shen, J. Y. Zhang, D. X. Zhao, B. S. Li, Y. M. Lu, Y. C. Liu, and X. W. Fan, J. Magn. Magn. Mater. **302**, 118 (2006).
[12] P. Sharma, A. Gupta, K. V. Rao, F. J. Owens, R. Sharma, R. Ahuja, J. M. O. Gullen, B. Johansson, and G. A. Gehring, Nature Mater. **2**, 673 (2003).
[13] W. Chen, L. F. Zhao, Y. Q. Wang, J. H. Miao, S. Liu, Z. C. Xia, and S. L. Yuan, Appl. Phys. Lett. **87**, 42507 (2005).
[14] V. K. Sharma, R. Xalxo, and G. D. Varma, Cryst. Res. Technol. **42**, 34 (2007).
[15] W. G. Carlson and T. K. Gupta, J. Appl. Phys. **53**, 5746 (1982).
[16] S. Deka and P. A. Joy, Solid State Commun. **142**, 190 (2007).
[17] C. Kato, K. Kuroda, and K. Hasegawa, Clay Minerals **14**, 13 (1979).
[18] D. J. Priour Jr., E. H. Hwang, and S. D. Sarma, Phys. Rev. Lett. **92**, 117201 (2004).
[19] V. K. Sharma and G. D. Varma, Cryst. Res. Technol. **43**, 1046 (2008).

DOI:10.1088/1674-0068/23/04/469-472 